



## Mechanisms of Miscible and Immiscible scCO<sub>2</sub> Displacement Efficiency: Analytical Evaluation of Experimental conditions

Doaa Saleh Mahdi<sup>1\*</sup>, Duraid Al-Bayati<sup>2,3</sup>, Ali Saeedi<sup>2</sup>, Mathew Myers<sup>4</sup>, Cameron White<sup>4</sup>

<sup>1</sup>Petroleum Technology Department, University of Technology-Iraq

<sup>2</sup>Curtin University, 26 Dick Perry Avenue, Kensington, WA 6151, Australia

<sup>3</sup>University of Kirkuk, College of Engineering, Petroleum Engineering Department, Kirkuk, Iraq, 6300

<sup>4</sup>CSIRO-Energy, 26 Dick Perry Avenue, Kensington, WA 6151, Australia

### Article information

#### Article history:

Received: January, 16, 2022

Accepted: February, 25, 2022

Available online: April, 8, 2022

#### Keywords:

CO<sub>2</sub> EOR,  
Miscible displacement,  
Immiscible displacement,  
Dimensionless analysis.

#### \*Corresponding Author:

Doaa Saleh Mahdi

[150082@uotechnology.edu.iq](mailto:150082@uotechnology.edu.iq)

### Abstract

CO<sub>2</sub> injection has proven to be one of the most successful EOR (Enhanced Oil Recovery) methods, as compared with other injection gases CO<sub>2</sub> miscibility with oil is easier to achieve. During gas injection into reservoirs, oil might be bypassed on either a micro- or macroscopic scale because of different types of heterogeneities. In this work, the performance of first-contact-miscible (FCM) and immiscible (IM) CO<sub>2</sub> injections were investigated experimentally using outcrop sandstone core samples. Decane was also used as the hydrocarbon phase as it has a relatively low minimum miscibility pressure (MMP) with CO<sub>2</sub> (12.4 MPa). Core flooding experiments were conducted at two pressures of 17.2 MPa and 9.6 MPa and the common temperature of 343 K. Furthermore, analytical calculations of dimensionless numbers are used to study the dominant forces and mechanisms which are correlated with the results of the core flooding experiments. The impacts of gravity, swelling and vaporization on the end results were inferred from the oil recoveries, variations in the pore pressure and dimensional analysis. For CO<sub>2</sub> injection in homogeneous core samples, a maximum recovery of 93.5% and 76% was achieved for the FCM and IM displacements, respectively. The higher recovery results of FCM is attributed to the vanishing capillary pressure between displacing and displaced phases. Dimensional analysis showed that the flow is at the capillary-gravity equilibrium at immiscible conditions, while there is dominance of gravity-viscous forces at miscible conditions.

## 1. Introduction

The investigation into the use of CO<sub>2</sub> flooding for enhanced oil recovery (EOR) began in the early 1950's [1-3] and has since been considered as one of the most efficient EOR methods. Furthermore, injecting CO<sub>2</sub> has captured more interest in the recent years as it can help to reduce CO<sub>2</sub> gas emissions [4-18]. Various studies have been performed to improve the understanding of CO<sub>2</sub> flow through porous media [19-29]. However, the efficiency of a CO<sub>2</sub> EOR greatly depends on whether the in-situ displacement occurs under immiscible, near-miscible, or miscible conditions.

### 1.1. Effect of Miscibility

In an immiscible (IM) flooding process, the high-density difference between injected CO<sub>2</sub> and oil and high-mobility ratio can lead to poor macroscopic sweep efficiency by promoting viscous fingering and gravity segregation, keeping the recovery factor low [30-32]. It is also widely acknowledged that improving the microscopic and/or macroscopic sweep efficiencies is the key for the success and effectiveness of any EOR technique [33].

The CO<sub>2</sub> miscibility with the in-situ oil is achieved if the flooding pressure is higher than the so-called minimum miscibility pressure (MMP) under reservoir conditions. The interactions between CO<sub>2</sub> and oil at high pressures (higher than MMP) are much stronger than those at low pressures [34, 35]. When miscibility between the injected gas and oil is achieved a high recovery factor may result. Miscible gas injection generally results in a higher microscopic displacement efficiency by lowering the interfacial tension (IFT) between the oil and CO<sub>2</sub>, causing oil swelling and lowering the oil viscosity and density [34-36]. The above effects are mainly due to the mass transfer that takes place in a miscible CO<sub>2</sub> displacement [37].

### 1.2. Dimensionless analysis

Dimensionless analysis has been found to be a powerful tool for better understanding of the effects of simultaneous phenomena that may occur during fluid flow in a porous medium [38-40]. In other words, combining the experimental results with dimensionless calculations can assist in indicating the dominant recovery mechanisms and relative significance of active forces (i.e. capillary, viscous and gravitational) during a miscible or an immiscible flooding process. Described below are some of the commonly used dimensionless parameters used to characterise multiphase displacements in the porous media.

As outlined by (1), the capillary number [41], describes the relationship between viscous and capillary forces.

$$N_c = (\text{Viscous forces})/(\text{Capillary forces}) = (v \mu)/IFT \quad (1)$$

where,  $v$  is the Darcy velocity (m/s),  $\mu$  is the viscosity of displacing phase (Pa s) and IFT is the interfacial tension between the displacing and displaced fluids (N/m). The capillary number is of the order of about  $10^{-7}$  for common immiscible fluid injections [39].

The bond number [39] is a measure of the ratio of gravity to capillary forces and is quantified by (2).

$$N_b = (\text{Gravity forces})/(\text{Capillary forces}) = (\Delta\rho g D_h^2)/IFT \quad (2)$$

where,  $\Delta\rho$  is the density contrast between displacing and displaced fluids ( $\text{kg/m}^3$ ),  $g$  is the gravity constant ( $\text{m/s}^2$ ) and  $D_h$  is the hydraulic diameter of pores (m). The bond number is in the order of about  $10^{-4}$  for common immiscible flooding processes [39].

The gravity number [42] is used to quantify the ratio between the gravity and viscous forces as defined by (3).

$$N_g = (\text{Gravity forces})/(\text{Viscous forces}) = (\Delta\rho g k)/(v\mu) \quad (3)$$

In addition to those reviewed so far, Zhou et al. (1994) [43] introduced other dimensionless numbers to describe fluid flow at the core-scale level. As defined by these researchers, the relative magnitude of capillary to viscous forces can be estimated from the following relationship:

$$N_{cv} = (\text{Capillary forces})/(\text{Viscous forces}) = (D k P_c)/(v L^2 \mu) \quad (4)$$

where,  $k$  is the average permeability ( $\text{m}^2$ ),  $P_c$  is the capillary pressure (Pa) and  $L$  is the sample or reservoir length (m). When  $N_{cv}$  varies between 0.2 and 5.0, capillary and viscous forces are of the same order of magnitude. If it is above 5.0 or below 0.2 that the capillary or viscous forces are dominant, respectively [43].

Similarly, Zhou et al. (1994) [43] define the ratio of capillary to gravity force using (5).

$$N_{cg} = (\text{Capillary forces})/(\text{Gravity forces}) = P_c/(H \Delta\rho g) \quad (5)$$

where,  $H$  is the reservoir or sample thickness (m) and  $\Delta\rho$  is the density difference between displaced and displacing fluids ( $\text{kg/m}^3$ ).

The same researchers expressed that the ratio of gravity to viscous force is with  $N_{gr}$  that can be estimated using (6).

$$N_{gr} = (\text{Gravity forces})/(\text{Viscous forces}) = (\Delta\rho g D_h K)/(L v \mu_o) \quad (6)$$

This research is aimed at providing a better understanding of the displacement mechanisms during miscible and immiscible  $\text{CO}_2$  injection and how they may influence the ultimate oil recovery. For this purpose, we have performed a series of core-flooding experiments under two different pressure conditions, one above and another below MMP of the  $\text{CO}_2$  into decane as the fluid system of interest. We have also demonstrated how the

calculations of dimensionless numbers at the pore- and core-scale levels may be used to determine the dominant forces and mechanisms during the flooding experiments.

## 2. Experimental Approach

### 2.1. Core Flooding Equipment

A moderate pressure and temperature core flooding facility was built for the CO<sub>2</sub> flooding experiments planned. The flow diagram of the experimental setup is shown in (Fig. 1). The setup consisted of a hydrostatic type core holder (69 MPa and 473 K rated) and three Teledyne Isco syringe pumps (69 MPa rating) used for controlling confining and pore pressure. A high pressure N<sub>2</sub> cell was also used to control the back pressure which was applied using a dome-loaded backpressure regulator (BPR) during the experiments. Two 316 stainless steel transfer cylinders were used for storing and injecting decane and CO<sub>2</sub>, while the synthetic formation brine was injected directly using a syringe pump. Two absolute pressure transducers (Omega Engineering, PX309-2KG5V) were installed on the inlet and outlet of the core-holder for differential pressure measurement. Experiments were conducted at 343 K and two pressures of 17.23 MPa and 9.65 MPa to ensure experiments were representative of first contact miscible (FCM) and IM reservoir conditions (the MMP between decane and CO<sub>2</sub> is 12.4 MPa at 343 K as reported by (Shaver et al., 2001 and Georgiadis et al., 2010).

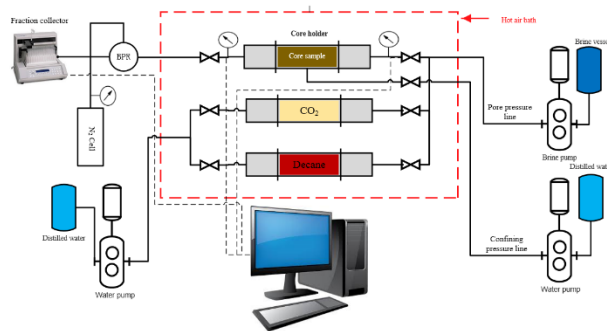


Fig. 1. Schematic drawing of core flooding apparatus

### 2.2. Experimental material

High purity CO<sub>2</sub> (99.9 wt%, BOC Gases), *n*-Decane (99%, Sigma–Aldrich), and a synthetic brine consisting of 2% NaCl, 0.7% KCl, 0.5% CaCl<sub>2</sub>.H<sub>2</sub>O, (all in weight%, ACS grade, Sigma–Aldrich) dissolved in distilled water, were used in the experiments. Two outcrop sandstone samples (Upper Gray Berea) each with a length of 7.65 cm, diameter of 3.81 cm and 100 md of permeability were used as the porous medium. The fluid properties under different experimental conditions applied are provided in Table 1.

Table 1. Fluid properties under various pressures

P (MPa)	CO <sub>2</sub> <sup>*</sup>		Decane <sup>*</sup>		IFT <sup>**</sup> (mN/m <sup>2</sup> )
	ρ (kg/m <sup>3</sup> )	μ (cp)	ρ (kg/m <sup>3</sup> )	μ (cp)	

9.65	233	0.022	700.9	0.545	3.55
17.23	590	0.045	707.7	0.591	0

\*NIST Chemistry WebBook, SRD 69, 2017.

### 2.3. Experimental material

Before each core-flooding experiment, a core plug was cleaned in a temperature controlled Dean-Stark apparatus using warm methanol and toluene (50% each) and then dried in a vented oven at 343 K for 24 hours or until its weight stabilized. Then, the core sample was wrapped with a layer of FEP heating shrinkage tube, and placed in a Viton sleeve (this layer was required to prevent any CO<sub>2</sub> diffusion and damage to the Viton sleeve). Subsequently, the sleeve containing the sample was installed into the core-holder (placed horizontally). In the next step, the confining pressure was set at 17.23 MPa, while the core sample was vacuumed to  $7 \times 10^{-4}$  psi over 12 hours. The brine flooding was then started to saturate the core sample and apply the pore pressure, while the confining pressure was gradually increased to 34.47 MPa by maintaining a net value of 17.23 MPa between the overburden pressure and pore pressure. After fully saturating the core sample (placing the system under a constant pore pressure of 13.78 MPa for 6 hours or until pore pressure became stable) the brine permeability was measured. Subsequently, about five pore volumes (PV) of decane were injected at 5 mL/min (i.e. a capillary number of  $< 10^{-4}$ ) to achieve connate water saturation ( $S_{wc}$ ). Eventually, CO<sub>2</sub> was injected at a flow rate of 0.5 cc/min (determined using the [44] criterion of  $L\mu v \geq 1 - 5$ , where  $L$  is the core length (m),  $v$  is the flow velocity (m/s), and  $\mu$  is the viscosity of the displacing fluid (Pa s)). In addition, the volume of decane collected for each PV of CO<sub>2</sub> was recorded. The flooding was continued till 2-2.5 PV's of CO<sub>2</sub> were injected.

## 3. Results and Discussion

### 3.1. Core Flooding Experiments

We performed two different CO<sub>2</sub> injection tests each at a different pressure (one below and another above the MMP of CO<sub>2</sub> into decane at 343 K) on homogeneous core samples to determine the influence of miscibility and active forces at the pore- and core-scale on the oil recovery. Decane recoveries of 93.5% and 76% were achieved for the miscible and immiscible displacements, respectively. Fig. 2 shows the dynamic decane recovery of both experiments versus PV's of CO<sub>2</sub> injected. As can be seen, the recovery during immiscible displacement grows faster during the times leading to CO<sub>2</sub> breakthrough. One reason for this behaviour is the faster flow of gas inside the core sample during immiscible injection which takes place through the preferential paths (i.e. flow fingers) that present the least resistance to flow [45]. For instance, the injected CO<sub>2</sub> invades the larger pores first [41] pushing the oil towards the production side of the core. On the other hand, a continuous mixing process

(vaporisation and condensation) would take place between fluid phases under miscible conditions giving rise to a more uniform displacement front and a delay in CO<sub>2</sub> breakthrough. After CO<sub>2</sub> breakthrough, not much decane can be recovered in the case of immiscible flooding but for miscible condition, decane is recovered with a relatively moderate rate even after breakthrough contributing towards a higher eventual recovery (Fig. 2). The main cause of this behaviour is that during the immiscible displacement, once the preferential flow paths are established and breakthrough occurs, due to the dominance of capillary forces, not much additional oil may be recovered. In the case of the miscible flooding however, the capillary forces do not exist resulting in an eventual recovery close to 100%. Moreover, the measured pressure data during the tests (Fig.3) indicate lower differential pressures during the miscible displacement, which is due to the vanishing interfacial tension under miscible conditions, but two phase flow occurs during the immiscible flooding where capillary forces are active giving rise to higher differential pressures.

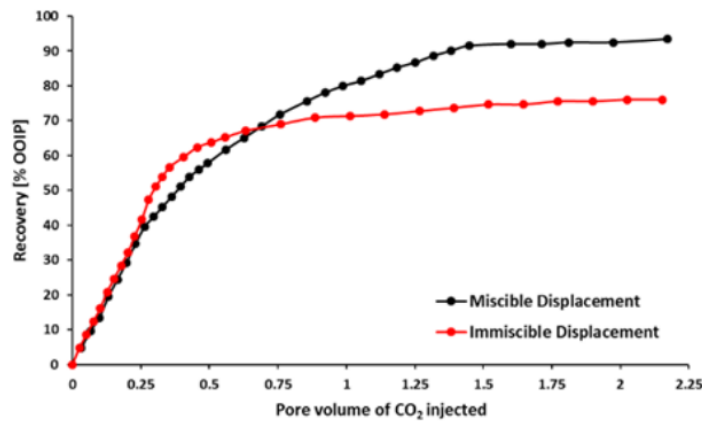


Fig. 2. Dynamic recovery at different miscibility conditions

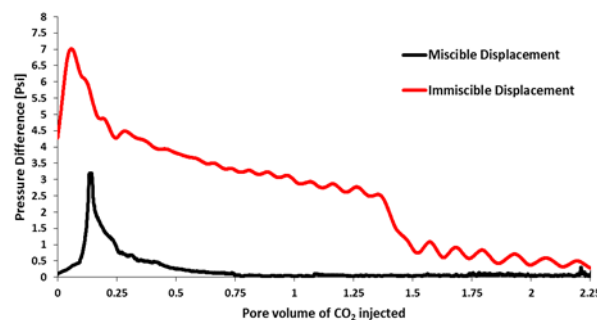


Fig. 3. Dynamic record of differential pressure

### 3.2. Core Flooding Experiments

Combining the result of the displacement experiments with dimensionless calculations can assist in determining the dominant recovery mechanisms and relative significance of likely active forces during the displacements. The calculated values of the capillary, bond and gravity numbers for our experiments are presented in Table 2. The hydraulic diameter used in calculating these parameters was calculated according to

the technique proposed by Epstein (1989) [46]. As can be seen from Table 2, under immiscible conditions (pore pressure of 9.65 MPa), the capillary and bond numbers are within the expected range for flooding experiments as reported in the literature (Capillary number is about  $10^{-7}$  and the bond number is about  $10^{-2}$ ) [39]. As the IFT approaches zero under the miscible conditions (pore pressure of 17.23 MPa) these numbers grow toward the critical point (i.e. infinity).

At the core-scale level [46], the capillary pressure was calculated for our experiments using a history matching technique conducted using the Sendra software package (Weatherford Petroleum Consultants). Then corresponding values of  $N_{cv}$ ,  $N_{cg}$  and  $N_{gv}$  (as defined by equations 4, 5 and 6) were calculated (Table 3) providing insights as to which forces would dominant during each of the two experiments. For instance, under immiscible conditions, during the first stage of flooding, under the effect of capillary and viscous forces CO<sub>2</sub> invades the larger pores first but as the injection continues the gravity forces may become more pronounced and the CO<sub>2</sub> moves preferentially into the least resistance paths [41]. On the other hand, the absence of the capillary forces during miscible displacement would lead to the dominance of viscous forces during the flood as well as the existence of a non-negligible effect of gravity forces.

Table 2. Pore-dimensionless

P (MPa)	$N_c$	$N_b$	$N_g$
9.65	2.25E-07	5.21E-02	2.82E+00
17.23	Infinity	Infinity	3.46E-01

scale calculations

Table 3. Core-scale dimensionless calculations

P (MPa)	$N_{cv}$	$N_{cg}$	$N_{gv}$
9.65	2.94E+00	1.32E+01	2.23E-01
17.23	0	0	5.18E-02

#### 4. Conclusions

To investigate and demonstrate the relative importance of active forces during CO<sub>2</sub> flooding, two experiments were conducted under miscible and immiscible conditions. In addition, dimensionless analysis was implemented at the pore- and core-scale to complement the results of the experiments. The following conclusions can be drawn upon combining the results of the experimental tasks and analytical investigations:

- As expected, a higher recovery was achieved from the first-contact-miscible test. This higher recovery is attributed to the vanishing interfacial tension between CO<sub>2</sub> and decane as well as the reduced density contrast between the two fluids.

- Before the CO<sub>2</sub> breakthrough, a higher oil production rate was achieved for the case of immiscible CO<sub>2</sub> displacement. This is attributed to the fast advancement of gas through the preferential flow paths that provide the least resistance to flow. In the miscible flood however the continuous vaporization and condensation of the fluid phases leads to a more stable displacement front and more gradual oil recovery even after breakthrough.
- Analytical calculations of dimensionless numbers revealed the existence of a capillary-gravity drive under immiscible conditions, while the gravity-viscous forces are dominant under miscible conditions.

## References

- [1] L. Whorton and W. Kieschnick, "A preliminary report on oil recovery by high-pressure gas injection," in *Drilling and Production Practice*, 1950: OnePetro.
- [2] L. P. Whorton, E. R. Brownscombe, and A. B. Dyes, "Method for producing oil by means of carbon dioxide," ed: Google Patents, 1952.
- [3] L. Holm, "Carbon dioxide solvent flooding for increased oil recovery," *Transactions of the AIME*, vol. 216, no. 01, pp. 225-231, 1959.
- [4] A. Saeedi, *Experimental study of multiphase flow in porous media during CO<sub>2</sub> Geo-Sequestration processes*. Springer Science & Business Media, 2012.
- [5] W. Ampomah *et al.*, "Optimum design of CO<sub>2</sub> storage and oil recovery under geological uncertainty," *Applied Energy*, vol. 195, pp. 80-92, 2017.
- [6] F. Kamali, F. Hussain, and Y. Cinar, "An experimental and numerical analysis of water-alternating-gas and simultaneous-water-and-gas displacements for carbon dioxide enhanced oil recovery and storage," *SPE Journal*, vol. 22, no. 02, pp. 521-538, 2017.
- [7] E. A. Al-Khdheawi, S. Vialle, A. Barifcani, M. Sarmadivaleh, and S. Iglauer, "Impact of reservoir wettability and heterogeneity on CO<sub>2</sub>-plume migration and trapping capacity," *International Journal of Greenhouse Gas Control*, vol. 58, pp. 142-158, 2017.
- [8] E. A. Al-Khdheawi, S. Vialle, A. Barifcani, M. Sarmadivaleh, and S. Iglauer, "Influence of injection well configuration and rock wettability on CO<sub>2</sub> plume behaviour and CO<sub>2</sub> trapping capacity in heterogeneous reservoirs," *Journal of Natural Gas Science and Engineering*, vol. 43, pp. 190-206, 2017.
- [9] E. A. Al-Khdheawi, S. Vialle, A. Barifcani, M. Sarmadivaleh, and S. Iglauer, "Influence of rock wettability on CO<sub>2</sub> migration and storage capacity in deep saline aquifers," *Energy Procedia*, vol. 114, pp. 4357-4365, 2017.
- [10] E. A. Al-Khdheawi, S. Vialle, A. Barifcani, M. Sarmadivaleh, and S. Iglauer, "Influence of CO<sub>2</sub>-wettability on CO<sub>2</sub> migration and trapping capacity in deep saline aquifers," *Greenhouse Gases: Science and Technology*, vol. 7, no. 2, pp. 328-338, 2017.
- [11] E. A. Al-Khdheawi, S. Vialle, A. Barifcani, M. Sarmadivaleh, and S. Iglauer, "Effect of wettability heterogeneity and reservoir temperature on CO<sub>2</sub> storage efficiency in deep saline aquifers," *International Journal of Greenhouse Gas Control*, vol. 68, pp. 216-229, 2018.
- [12] E. A. Al-Khdheawi, S. Vialle, A. Barifcani, M. Sarmadivaleh, and S. Iglauer, "Impact of injection scenario on CO<sub>2</sub> leakage and CO<sub>2</sub> trapping capacity in homogeneous reservoirs," in *Offshore Technology Conference Asia*, 2018: OnePetro.
- [13] E. A. Al-Khdheawi, S. Vialle, A. Barifcani, M. Sarmadivaleh, and S. Iglauer, "Impact of injected water

- salinity on CO<sub>2</sub> storage efficiency in homogenous reservoirs," *The APPEA Journal*, vol. 58, no. 1, pp. 44-50, 2018.
- [14] E. A. Al-Khdheawi, S. Vialle, A. Barifcani, M. Sarmadivaleh, and S. Iglauer, "The effect of WACO<sub>2</sub> ratio on CO<sub>2</sub> geo-sequestration efficiency in homogeneous reservoirs," *Energy Procedia*, vol. 154, pp. 100-105, 2018.
- [15] E. A. Al-Khdheawi, S. Vialle, A. Barifcani, M. Sarmadivaleh, and S. Iglauer, "Enhancement of CO<sub>2</sub> trapping efficiency in heterogeneous reservoirs by water-alternating gas injection," *Greenhouse Gases: Science and Technology*, vol. 8, no. 5, pp. 920-931, 2018.
- [16] E. A. Al-Khdheawi, S. Vialle, A. Barifcani, M. Sarmadivaleh, Y. Zhang, and S. Iglauer, "Impact of salinity on CO<sub>2</sub> containment security in highly heterogeneous reservoirs," *Greenhouse Gases: Science and Technology*, vol. 8, no. 1, pp. 93-105, 2018.
- [17] E. A. Al-Khdheawi, S. Vialle, A. Barifcani, M. Sarmadivaleh, and S. Iglauer, "Effect of the number of water alternating CO<sub>2</sub> injection cycles on CO<sub>2</sub> trapping capacity," *The APPEA Journal*, vol. 59, no. 1, pp. 357-363, 2019.
- [18] E. A. Al-Khdheawi, S. Vialle, A. Barifcani, M. Sarmadivaleh, and S. Iglauer, "Effect of brine salinity on CO<sub>2</sub> plume migration and trapping capacity in deep saline aquifers," *The APPEA Journal*, vol. 57, no. 1, pp. 100-109, 2017.
- [19] C. A. Fauziah, E. A. Al-Khdheawi, A. Barifcani, and S. Iglauer, "Wettability measurements of mixed clay minerals at elevated temperature and pressure: implications for CO<sub>2</sub> geo-storage," in *SPE Gas & Oil Technology Showcase and Conference*, 2019: OnePetro.
- [20] C. A. Fauziah, E. A. Al-Khdheawi, A. Barifcani, and S. Iglauer, "Wettability measurements on two sandstones: an experimental investigation before and after CO<sub>2</sub> flooding," *The APPEA Journal*, vol. 60, no. 1, pp. 117-123, 2020.
- [21] E. A. Al-Khdheawi, D. S. Mahdi, M. Ali, C. A. Fauziah, and A. Barifcani, "Impact of caprock type on geochemical reactivity and mineral trapping efficiency of CO<sub>2</sub>," in *Offshore Technology Conference Asia*, 2020: OnePetro.
- [22] C. A. Fauziah, E. A. Al-Khdheawi, S. Iglauer, and A. Barifcani, "Effect of Clay Minerals Heterogeneity on Wettability Measurements: Implications for CO<sub>2</sub> Storage," in *Offshore Technology Conference Asia*, 2020: OnePetro.
- [23] C. A. Fauziah, E. A. Al-Khdheawi, S. Iglauer, and A. Barifcani, "Influence of Total Organic Content on CO<sub>2</sub>-Water-Sandstone Wettability and CO<sub>2</sub> Geo-Storage Capacity," in *SPE Europec*, 2020: OnePetro.
- [24] C. A. Fauziah *et al.*, "Effect of CO<sub>2</sub> flooding on the wettability evolution of sand-stone," *Energies*, vol. 14, no. 17, p. 5542, 2021.
- [25] D. S. Mahdi, E. A. Al-Khdheawi, D. Al-Bayati, and C. Lagat, "Reservoir Fluids Model for a Middle Eastern Sandstone Reservoir," *Iraqi Journal of Oil & Gas Research*, vol. 1, no. 1, 2021.
- [26] E. A. Al-Khdheawi, C. A. Fauziah, D. S. Mahdi, and A. Barifcani, "A new approach to improve the assessments of CO<sub>2</sub> geo-sequestration capacity of clay minerals," in *International Petroleum Technology Conference*, 2021: OnePetro.
- [27] E. A. Al-Khdheawi, D. S. Mahdi, M. Ali, S. Iglauer, and A. Barifcani, "Reservoir scale porosity-permeability evolution in sandstone due to CO<sub>2</sub> geological storage," *Available at SSRN 3818887*, 2021.
- [28] C. A. Fauziah, E. A. Al-Khdheawi, C. Lagat, S. Iglauer, and A. Barifcani, "Influence of Gas Density on the Clay Wettability: Implication for CO<sub>2</sub> Geo-Sequestration," *Available at SSRN 3818907*, 2021.
- [29] C. A. Fauziah *et al.*, "Dependence of clay wettability on gas density," *Greenhouse Gases: Science and Technology*, vol. 11, no. 5, pp. 1066-1075, 2021.
- [30] D. Al-Bayati, A. Saeedi, C. White, Q. Xie, and M. Myers, "The Effects of Crossflow and Permeability

- Variation on Different Miscible CO<sub>2</sub> injection Schemes Performance in Layered Sandstone Porous Media," in *IOR 2019–20th European Symposium on Improved Oil Recovery*, 2019, vol. 2019, no. 1, pp. 1-10: European Association of Geoscientists & Engineers.
- [31] D. Al-Bayati, A. Saeedi, M. Myers, C. White, and Q. Xie, "An experimental investigation of Immiscible-CO<sub>2</sub>-Flooding efficiency in sandstone reservoirs: influence of permeability heterogeneity," *SPE Reservoir Evaluation & Engineering*, vol. 22, no. 03, pp. 990-997, 2019.
- [32] D. Al-Bayati *et al.*, "Evaluation of Miscible CO<sub>2</sub> WAG/Sandstone Interactions: Emphasis on the Effect of Permeability Heterogeneity and Clay Mineral Content," in *SPE Europec featured at 81st EAGE Conference and Exhibition*, 2019: OnePetro.
- [33] M. K. Verma, *Fundamentals of carbon dioxide-enhanced oil recovery (CO<sub>2</sub>-EOR): A supporting document of the assessment methodology for hydrocarbon recovery using CO<sub>2</sub>-EOR associated with carbon sequestration*. US Department of the Interior, US Geological Survey Washington, DC, 2015.
- [34] M. Ding, X.-A. Yue, H. Zhao, and W. Zhang, "Extraction and its effects on crude oil properties during CO<sub>2</sub> flooding," *Energy Sources, Part A: Recovery, Utilization, and Environmental Effects*, vol. 35, no. 23, pp. 2233-2241, 2013.
- [35] M. Nobakht, S. Moghadam, and Y. Gu, "Mutual interactions between crude oil and CO<sub>2</sub> under different pressures," *Fluid phase equilibria*, vol. 265, no. 1-2, pp. 94-103, 2008.
- [36] L. Holm and V. Josendal, "Mechanisms of oil displacement by carbon dioxide," *Journal of petroleum Technology*, vol. 26, no. 12, pp. 1427-1438, 1974.
- [37] F. M. Orr, *Theory of gas injection processes*. Tie-Line Publications Copenhagen, 2007.
- [38] R. Hilfer and P. Øren, "Dimensional analysis of pore scale and field scale immiscible displacement," *Transport in Porous Media*, vol. 22, no. 1, pp. 53-72, 1996.
- [39] M. Khosravi, A. Bahramian, M. Emadi, B. Rostami, and E. Roayaie, "Mechanistic investigation of bypassed-oil recovery during CO<sub>2</sub> injection in matrix and fracture," *Fuel*, vol. 117, pp. 43-49, 2014.
- [40] M. M. Kulkarni and D. N. Rao, "Experimental investigation of miscible and immiscible Water-Alternating-Gas (WAG) process performance," *Journal of Petroleum Science and Engineering*, vol. 48, no. 1-2, pp. 1-20, 2005.
- [41] C. Grattoni, X. Jing, and R. Dawe, "Dimensionless groups for three-phase gravity drainage flow in porous media," *Journal of Petroleum Science and Engineering*, vol. 29, no. 1, pp. 53-65, 2001.
- [42] M. Shook, D. Li, and L. W. Lake, "Scaling immiscible flow through permeable media by inspectional analysis," *In Situ;(United States)*, vol. 16, no. 4, 1992.
- [43] D. Zhou, F. Fayers, and F. Orr, "Scaling of multiphase flow in simple heterogeneous porous media," *SPE Reservoir Engineering*, vol. 12, no. 03, pp. 173-178, 1997.
- [44] L. Rapoport and W. J. Leas, "Properties of linear waterfloods," *Journal of Petroleum Technology*, vol. 5, no. 05, pp. 139-148, 1953.
- [45] C. Nutt, "The physical basis of the displacement of oil from porous media by other fluids: a capillary bundle model," *Proceedings of the Royal Society of London. A. Mathematical and Physical Sciences*, vol. 382, no. 1782, pp. 155-178, 1982.
- [46] N. Epstein, "On tortuosity and the tortuosity factor in flow and diffusion through porous media," *Chemical engineering science*, vol. 44, no. 3, pp. 777-779, 1989.